

$E0$ decay of the two first excited 0^+ states in ^{18}O

K. H. Souw, J. C. Adloff, D. Disdier, and P. Chevallier

Centre de Recherches Nucléaires, Université Louis Pasteur, Strasbourg, France

(Received 3 March 1975)

The reaction $^{19}\text{F}(t, \alpha)^{18}\text{O}$ has been used to study the $E0 \pi$ decays of the $^{18}\text{O}(3.63 \text{ MeV}, 0^+)$ and $^{18}\text{O}(5.33 \text{ MeV}, 0^+)$ states to the ground state. The $E0$ branching ratios Γ_π/Γ were measured to be, respectively, $(3.0 \pm 0.6) \times 10^{-3}$ and $\leq 2.3 \times 10^{-3}$. When these values are combined with the available lifetimes of these states, $E0$ matrix elements $\langle M \rangle_\pi = (6.0 \pm 0.7) \text{ fm}^2$ [$^{18}\text{O}(3.63 \text{ MeV})$] and $\leq 4.5 \text{ fm}^2$ [$^{18}\text{O}(5.33 \text{ MeV})$] are obtained. The properties of these states are compared to the theoretical predictions.

[NUCLEAR REACTIONS $^{19}\text{F}(t, \alpha)$, $E = 2.2 \text{ MeV}$; ^{18}O measured $E0$ branching ratios. Deduced $E0$ matrix elements.]

I. INTRODUCTION

It is interesting to study the ^{18}O nucleus with two neutrons outside an ^{16}O core. Of particular interest are the rather unknown structures of the low-lying excited 0^+ states at $E_x = 3.63$ and 5.33 MeV . The ^{18}O ground state (g.s.) is fairly well described as being nearly spherical with a dominant $(d_{5/2})^2$ structure, but it is unknown whether the second or third 0^+ state contains the larger component of core-excited configurations. This is because that before the particle-hole interaction is included, the second spherical and the first deformed 0^+ states are nearly degenerate. Because of uncertainties in the unperturbed positions, it is difficult to predict unambiguously which level is displaced up or down when the interaction is taken into account.¹ The $E2 \gamma$ -ray decay rate of the 3.63-MeV state lends evidence that this one is the more deformed level.² Coulomb shift analysis in mass 18 gives evidence for a predominantly $(s_{1/2})^2$ character of the 5.33-MeV state.³ However, from a knowledge of the $E0$ matrix elements, one can obtain independent and more direct information on the structural problem since the admixtures present in the two excited 0^+ states are directly related to those in the known g.s. configuration. Recently, Horsfjord,¹ by using the wave functions from the weak coupling model,^{2,4} calculated these matrix elements as a function of the unperturbed position of the $4p2h$ states relative to the $2p0h$ ones. By varying the relative position from $E = -1.5$ to 1.5 MeV , he found that the structure of the 0_2^+ state changes from being mainly deformed to being nearly spherical. The inverse behavior was found for the 0_3^+ state. On the other hand, the calculated $E0$ matrix elements vary significantly as a function of E . Therefore measure-

ments on the π decays involved permit a choice among possible structures. A comparison between various theoretical predictions for the structures of the two first excited 0^+ states is presented in Ref. 1.

A direct measurement of the $E0$ branching ratio (BR) of the 3.63-MeV state was performed by Gorodetzky *et al.*⁵ using proton inelastic scattering on an ^{18}O target and a magnetic spectrometer for the pair detection. They obtained $\Gamma_\pi/\Gamma = (1.9 \pm 0.4) \times 10^{-3}$. The mean lifetime of the 3.63-MeV state used in their work for calculating the $E0$ matrix element was $(3 \pm 1) \text{ psec}$ (Ref. 6). Since then more accurate lifetimes of $(1.45 \pm 0.25) \text{ psec}$ (Ref. 7) and $(1.33 \pm 0.20) \text{ psec}$ (Ref. 8) have been measured.

In this work we present the results of a new measurement on the $E0$ BR of the $^{18}\text{O}(3.63 \text{ MeV})$ state to g.s. together with the measurement of an upper limit for the π BR to the g.s. of the $^{18}\text{O}(5.33 \text{ MeV})$ state. We used the experimental method described in Ref. 9.

II. EXPERIMENTAL RESULTS

The $^{19}\text{F}(t, \alpha)^{18}\text{O}$ reaction, at an incident energy of 2.2 MeV , was used to excite the 0^+ states. The triton beam was delivered by the 3-MV Van de Graaff accelerator of the Centre de Recherches Nucléaires onto $100\text{-}\mu\text{g}/\text{cm}^2$ LiF targets evaporated on $40\text{-}\mu\text{g}/\text{cm}^2$ carbon backings. The high Q value of the reaction permitted the stopping of the elastically backscattered tritons in a $10\text{-}\mu\text{m}$ -thick aluminum foil while allowing the α particles to pass through and be detected in a $150\text{-mm}^2 \times 100\text{-}\mu\text{m}$ -thick surface barrier annular detector. Plastic scintillator telescopes with 0.2-mm -thick ΔE counters⁹ were used for the pair detection.

A. $^{18}\text{O}(3.63 \text{ MeV}, 0^+)(\pi)^{18}\text{O}(\text{g.s.})$ decay

The results of a 24-h measurement with a 100-nA beam current are represented in Figs. 1 and 2. Figure 1(a) is the direct singles α -particle spectrum. Figure 1(b) is the projection onto the α -particle energy axis of the two-dimensional α -particle energy versus π -energy spectrum (not represented) taken simultaneously with the spectrum of Fig. 1(a). Under the experimental conditions in which the data of Fig. 1(a) were taken, it was not possible to separate the α -particle groups feeding the 3.63- and 3.55-MeV states. However, this was done in a separate run by lowering the beam current to 50 nA, by reducing the target thickness to $40 \mu\text{g}/\text{cm}^2$, and by taking the direct spectra without the aluminum absorber in front of the annular detector. The part of this spectrum relevant to the 0^+ and 4^+ states is represented in the circle of Fig. 1(a). From this encircled spectrum we deduced the relative population of these two states in the other spectrum of Fig. 1(a).

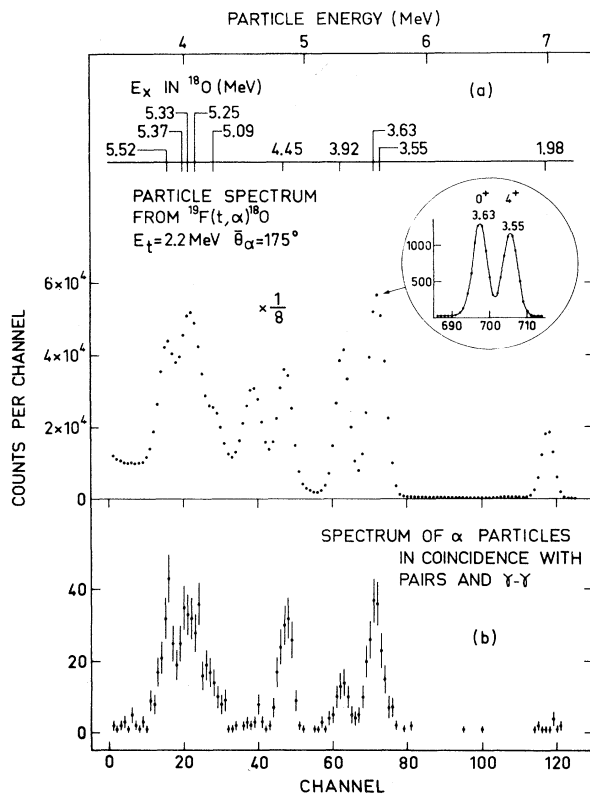


FIG. 1. (a) $\frac{1}{8}$ sampled direct α -particle spectrum from $^{19}\text{F}(t, \alpha)^{18}\text{O}$ taken simultaneously with the nonrepresented α -energy vs π -energy spectrum. The peak at channel 38 is from $^{16}\text{O}(t, \alpha)^{15}\text{N}(\text{g.s.})$. ^{16}O was a target contaminant. (b) Projection onto the α -energy axis of the two dimensional α -particle energy vs π -energy spectrum.

From the projection onto the pair energy axis of the two-dimensional spectrum in the α -particle channels 67–78, we deduced the g.s. π yield of the 3.63-MeV $E0$ decay. This projection is represented in Fig. 2(a). In subtracting the γ - γ interactions from the 0^+ and 4^+ γ -ray cascades via the 1.98-MeV state, the procedure given in Ref. 10 was used. We found 144 ± 17 pairs, which when

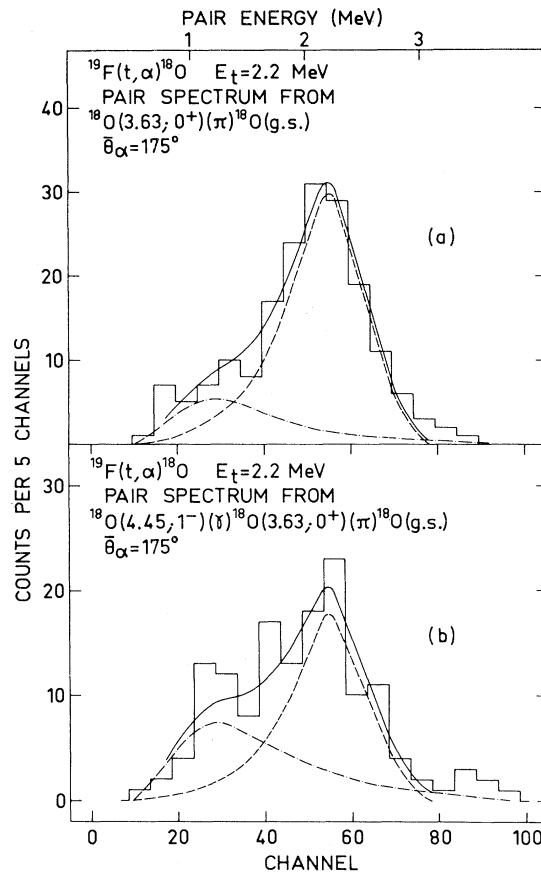


FIG. 2. (a) Pair spectrum obtained from the projection of events in channels 67–78 of Fig. 1(b) onto the π -energy axis of the relevant α -energy vs π -energy spectrum (not represented). The dashed-dotted line is the shape of the γ - γ interactions in the telescope due to γ -ray decays of the unresolved 3.55- and 3.63-MeV states. The dashed line is the shape of the π spectrum from the 3.63 MeV \rightarrow g.s. π decay deduced from the $^{40}\text{Ca}(3.35 \text{ MeV}) \rightarrow$ g.s. π decay. The weighting of these two curves was obtained by a least squares fit. The number of γ - γ interactions (dashed-dotted curve) is in good agreement with that calculated by using $(1.5 \pm 0.3) \times 10^{-5}$ γ - γ interactions per detected particle (Refs. 9 and 10). (b) Pair spectrum obtained from the projection of events in channels 43–54 of Fig. 1(b) onto the π -energy axis of the two-dimensional spectrum. The dashed-dotted line is the shape of the γ - γ interactions due to the γ -ray cascades $4.45 \text{ MeV} \rightarrow 1.98 \text{ MeV} \rightarrow$ g.s. and $4.45 \text{ MeV} \rightarrow 3.63 \text{ MeV} \rightarrow 1.98 \text{ MeV} \rightarrow$ g.s. The dashed line is the π -spectrum shape from the 3.63 MeV \rightarrow g.s. π decay.

combined with the 0^+ α -particle yield in channels 67–78 of Fig. 1(a) and the calculated π efficiency,⁹ gives $\Gamma_\pi/\Gamma = (3.0 \pm 0.6) \times 10^{-3}$ for the 3.63-MeV state.

The occurrence of the $^{18}\text{O}(4.45 \text{ MeV}, 1^-)$ peak in both our singles and coincidence spectra allowed us to calculate Γ_π/Γ from the number of observed pairs from the 0^+ state in coincidence with the α -particles feeding the 4.45-MeV state. These coincidences, which are shown in Fig. 2(b), originate in the γ -ray cascade from the 1^- level to the 0^+ level. From Refs. 8, 11–14 we deduce $(70 \pm 3)\%$ for the mean weighted value of this γ -ray BR. When combined with the π yield in Fig. 2(b), the α -particle yield for the 1^- level in Fig. 1(a), and the calculated π efficiency, this yields $\Gamma_\pi/\Gamma = (2.7 \pm 0.8) \times 10^{-3}$ for the 3.63-MeV state.

By taking the more precise value $\Gamma_\pi/\Gamma = (3.0 \pm 0.6) \times 10^{-3}$ as our final result and the weighted lifetime $\tau_m = (1.39 \pm 0.16)$ psec deduced from Refs. 7 and 8 the partial π lifetime of the 3.63-MeV state in ^{18}O is found to be $\tau_\pi = (0.46 \pm 0.11)$ nsec. The value of the monopole matrix element deduced from τ_π is $(6.0 \pm 0.7) \text{ fm}^2$.

B. $^{18}\text{O}(5.33 \text{ MeV}, 0^+) (\pi) ^{18}\text{O}(\text{g.s.})$ decay

Figure 3 displays that part of the good resolution α -particle spectrum corresponding to the region in channels 10–33 of the spectrum in Fig. 1(a).

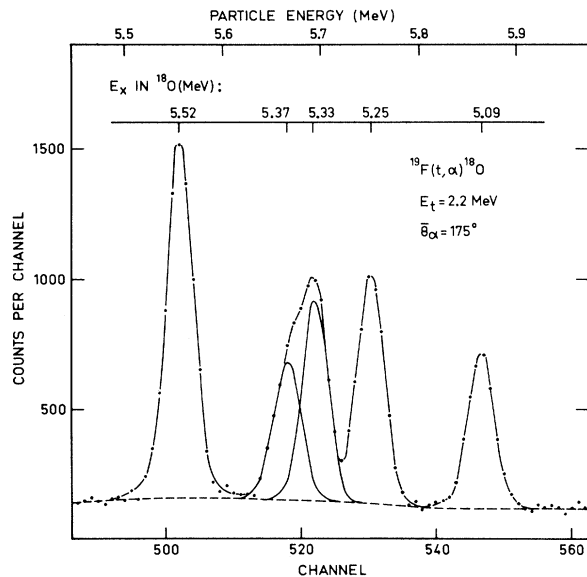


FIG. 3. Partial direct α -particle spectrum from $^{19}\text{F}(t, \alpha)^{18}\text{O}$. The dashed line is the adopted background. The decomposition of the doublet into peaks at 5.33 and 5.37 MeV was obtained by a least squares fit using the shape of the α -particle peak relevant to the 3.92-MeV state.

The decomposition into two components of the peak around channel 520 of Fig. 3 is the result of a least squares fit and was done to obtain the yield of the 5.33-MeV state in the spectrum of Fig. 1(a). The spectrum shown in Fig. 4 is the projection onto the π -energy axis of the events in channels 17–27 of Fig. 1(b) in which region occurs the 5.33-MeV to g.s. $E0$ decay. The spectrum shape in Fig. 4 is largely due to γ - γ interactions from cascades of the 5.37-, 5.33-, and 5.25-MeV states, to a smaller extent to those from the 5.52- and 5.09-MeV states, and to $E0$, $E1$, $M1$, and $E2$ internal pairs with transition energies between 3.27 and 3.63 MeV from the various decay modes. The $(35 \pm 2)\%$ g.s. γ -ray decay^{12–16} of the 5.25-MeV state produces an $E2$ internal π yield of nearly the same energy as the 5.33-MeV $E0$ decay. This $E2$ π yield was calculated⁹ to be 33 ± 7 pairs in the spectrum of Fig. 4. In order to determine the shape of the spectrum of pairs of ≈ 4.3 -MeV total kinetic energy, we measured the internal pairs from the 5.27- and 5.30-MeV states in ^{15}N by using the $^{18}\text{O}(p, \alpha)^{15}\text{N}$ reaction at $E_p = 5.63$ MeV. This shape was used in drawing the dashed curve in Fig. 4 which represents the spectrum that would result from a 2.3×10^{-3} g.s. $E0$ π BR for the 5.33-MeV state in ^{18}O . In calculating this BR we subtracted the $E2$ π yield of the 5.25-MeV g.s. decay from the yield of the dashed curve in Fig. 4. We take the value 2.3×10^{-3} as an upper limit for the BR of the 5.33-MeV state to g.s. When this upper limit is combined with the lower value of the lifetime $\tau_m = (0.20 \pm 0.04)$ psec⁸ the corresponding matrix element is $\langle M \rangle_\pi \leq 4.5 \text{ fm}^2$. The tail beyond channel 80 appearing in the histogram of Fig. 4 is attributed mainly to interactions in the telescopes

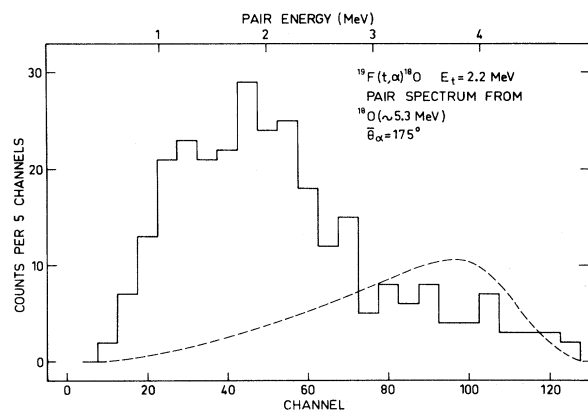


FIG. 4. Pair spectrum obtained from the projection of events in channels 17–27 of Fig. 1(b) onto the π -energy axis of the two-dimensional spectrum. The dashed line is the shape of the π spectrum from the 5.33 MeV \rightarrow g.s. π decay deduced from the $^{15}\text{N}(\sim 5.3 \text{ MeV}) \rightarrow$ g.s. π decay.

TABLE I. Some properties of the two first excited $J^\pi = 0^+$ states in ^{18}O .

E_x (MeV)	τ_m (psec)	Γ_π/Γ	$\langle M \rangle_\pi$ (fm 2)	$E0$ strength (single particle units) ^a
3.63	1.39 ± 0.16^b	$(3.0 \pm 0.6) \times 10^{-3}$	6.0 ± 0.7	1.8 ± 0.4
5.33	0.20 ± 0.04^c	$\leq 2.3 \times 10^{-3}$	≤ 4.5	≤ 1

^a See Ref. 23.^b Mean weighted value deduced from Refs. 7 and 8.^c See Ref. 8.

resulting from multiple cascading. This tail is also present in the projections (not shown) in α channels 11–16 (5.52 MeV state) and in channels 29–32 (5.09 MeV state) for which high energy internal π emissions are negligibly small. Thus the true value of the π BR of the 5.33-MeV state might be far smaller than 2.3×10^{-3} .

Table I summarizes the present results together with the lifetimes used in calculating the $E0$ matrix elements.

III. DISCUSSION

The value for the π BR of the 3.63-MeV state obtained in Ref. 5 (see Sec. I) is some 40% smaller than our value (Table I). In that experiment⁵ the yield of the γ -ray decay of the 3.63- to the 1.98-MeV state, measured with a NaI detector, was used as a normalization with no account taken of possible feeding of the 4^+ state at 3.55 MeV. We made a p - γ coincidence measurement with a Ge-Li detector at $\theta_\gamma = 55^\circ$, $\theta_p = 180^\circ$ using the $^{18}\text{O}(p, p')$ reaction at $E_p = 5.63$ MeV. This measurement shows that for these angles and bombarding energy, it is mainly the 4^+ state which is populated. At their bombarding energy which was 300 keV lower, the population of the 4^+ state could have been different. However, a contribution of this state in their normalizing γ -ray spectra was still possible and could explain the difference in the two π -BR results.

The present values and other experimental results such as those obtained in electron inelastic scattering by Groh *et al.*¹⁷ will now be discussed in the framework of the calculations of Horsfjord.¹ In the case of electron inelastic scattering, Horsfjord calculated the theoretical nuclear form factors and the quantity $\lim_{q \rightarrow 0} \{ [B(C0, q)]^{1/2} / q^2 \}$ as a function of the parameter E for the $0_1^+ \rightarrow 0_2^+$ and $0_1^+ \rightarrow 0_3^+$ excitations in ^{18}O . In the limit, $B(C0, q)$ is the electric monopole reduced transition probability from the g.s. to the excited state for a transferred momentum q .¹⁸ From his form factors we deduced the $B(C0, q)$ values and the values of the theoretical $E0$ matrix elements by using the

relation^{18,19}:

$$\lim_{q \rightarrow 0} \{ [B(C0, q)]^{1/2} / q^2 \} = \langle M \rangle_\pi / (6 \times \sqrt{4\pi}). \quad (1)$$

In Fig. 5(b) are represented the values of these $E0$ matrix elements for the $0_2^+ \rightarrow 0_1^+$ and $0_3^+ \rightarrow 0_1^+$ π

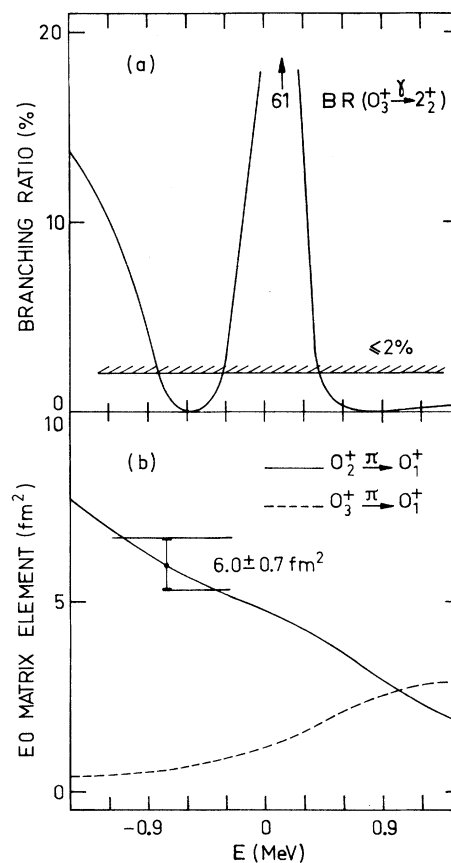


FIG. 5. (a) Theoretical BR deduced from Ref. 1 for the $E2$ $0_3^+ \rightarrow 2_2^+$ γ -ray decay in ^{18}O as a function of the energy shift E , assuming the sum $\text{BR}(0_3^+ \rightarrow 2_2^+) + \text{BR}(0_3^+ \rightarrow 2_1^+) = 61\%$ (Ref. 13). The experimental upper limit of 2% (Ref. 13) is the horizontal line. (b) $E0$ matrix elements deduced from Ref. 1 for the $0_2^+ \rightarrow 0_1^+$ and $0_3^+ \rightarrow 0_1^+$ π decays as a function of E . The experimental point is the experimental value of (6.0 ± 0.7) fm 2 deduced in this work.

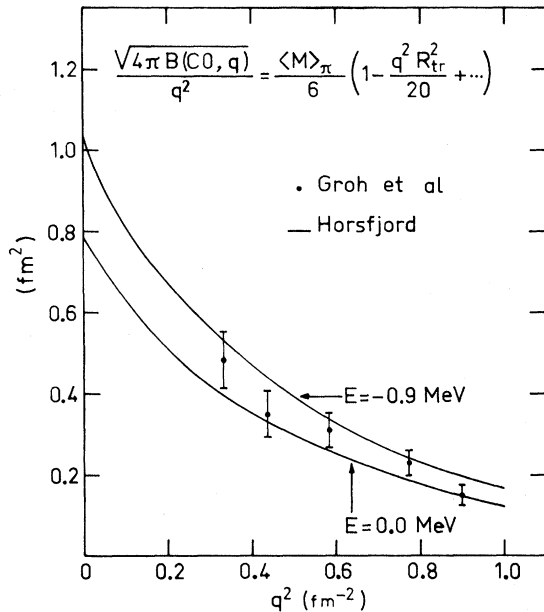


FIG. 6. The quantities $[4\pi B(C0, q)]^{1/2}/q^2$ as a function of q^2 (see Sec. III) deduced from Ref. 1 for $E = 0.0$ and -0.9 MeV (solid lines) for the $0_1^+ \rightarrow 0_2^+$ excitations. $R_{tr}^2 = \langle 0_2^+ | \Sigma_p r_p^4 | 0_1^+ \rangle / \langle 0_2^+ | \Sigma_p r_p^2 | 0_1^+ \rangle$ (Refs. 18 and 19). The experimental points are deduced from the form factors measured in the work of Groh *et al.* (Ref. 17).

decays. The matrix elements deduced in our work for the $0_2^+ \rightarrow 0_1^+$ π decay is reported in the figure. It indicates $-1.2 \leq E \leq -0.4$ MeV. In Fig. 6 we represent the experimental quantities $[4\pi B(C0, q)]^{1/2}/q^2$ deduced from the form factors of Groh *et al.*¹⁷ for the $0_1^+ \rightarrow 0_2^+$ excitation together with the theoretical curves¹ for $E = 0.0$ and -0.9 MeV. As can be seen here too, a negative value for E is predicted ($0.0 \leq E \leq -0.9$ MeV). Thus, in agreement with the calculations of Horsfjord, an $E0$ matrix element lying between the limits $4.7 \lesssim \langle M \rangle_\pi \lesssim 6.4$ fm^2 can be deduced for $q^2 = 0.0$ fm^{-2} in the figure.

Another interesting quantity to deal with is the γ -ray BR of the third 0^+ state to the second 2^+ state. Horsfjord calculated this ratio as a function of E and adopted a value of $(10 \pm 5)\%$ (Ref. 6) in his discussion. Later, however, upper limits of 2% (Ref. 13) and 5% (Ref. 8) were given for this γ -ray decay. The curve in Fig. 5(a) represents the variations of the $0_3^+ \rightarrow 2_2^+$ γ -ray BR as a function of E . In deducing this curve from Ref. 1 we took $\text{BR}(0_3^+ \rightarrow 2_1^+) + \text{BR}(0_3^+ \rightarrow 2_2^+) = 61\%$, the value

given by Berant *et al.*¹³ Their upper limit of 2% for $\text{BR}(0_3^+ \rightarrow 2_2^+)$ is reported in the figure. It indicates that the parameter E is restricted to $-0.8 \leq E \leq -0.3$ MeV or $E \geq 0.4$ MeV.

If one takes $E = -0.75$ MeV as the energy difference of the $4p2h$ and $2p0h$ states, in agreement with the results of Figs. 5 and 6, the wave functions of the 3.63- and 5.33-MeV states include, respectively, 82% of $4p2h$ excitations and 91% of $2p0h$ excitations according to Horsfjord. Therefore one might conclude that the 3.63-MeV state is the most deformed among the three first 0^+ states in ^{18}O , a conclusion which, as mentioned earlier, is also supported by the $E2$ rate of the 3.63-MeV state.²

If one adopts the value $E = -0.75$ MeV, the predicted theoretical value for the matrix element of the 5.33-MeV $E0$ decay to g.s. is $\langle M \rangle_\pi = 0.7$ fm^2 [Fig. 5(a)]. By taking $\tau_\pi = (0.20 \pm 0.4)$ psec for the lifetime of the state,⁸ the π BR would be $\Gamma_\pi/\Gamma = 4.0 \times 10^{-5}$ which could be hardly measurable with our technique. This value is considerably smaller than the upper limit we were able to put on this π decay (Table I). However, as stated in Sec. IIB, a lower value is likely for the π BR of the 5.33-MeV state. Unfortunately, in Ref. 17 too, it was not possible to make a valid comparison with the predictions of Benson and Irvine²⁰ and the experimental (e, e') form factors. Their predictions for the $E0$ matrix element are approximately the same as those of Horsfjord¹ if Woods-Saxon radial wave functions are used in their calculation in place of harmonic oscillator ones. Woods-Saxon radial wave functions in effect raise the value of the matrix elements.²¹

Although no definite conclusion about the value of the $E0$ matrix element on the 5.33-MeV state could be given in either our work or in the (e, e') measurements,¹⁷ the good agreement of observation with prediction for the 3.63-MeV state makes it reasonable to suppose that the 5.33-MeV level is a good candidate for the nearly spherical ($s_{1/2}$)² 0_3^+ state predicted in Refs. 1, 4, 20, and 22. This assumption is also supported by the small γ -ray BR ($0_3^+ \rightarrow 2_2^+$) and by the Coulomb shift analysis in mass 18 (Ref. 3). It would be interesting to measure this $E0$ matrix element in low momentum transfer (e, e') experiments.

We would like to thank A. Pape for critically reading the manuscript.

- ¹V. Horsfjord, Nucl. Phys. A209, 493 (1973).
²T. Engeland and P. J. Ellis, Nucl. Phys. A181, 368 (1972).
³A. V. Nero and E. G. Adelberger, Phys. Rev. Lett. 32, 623 (1974).
⁴P. J. Ellis and T. Engeland, Nucl. Phys. A144, 161 (1970).
⁵S. Gorodetzky, R. E. Pixley, A. Gallmann, G. Frick, J. P. Coffin, and G. Sibille, J. Phys. (Paris) 24, 892 (1963).
⁶A. E. Litherland, M. J. L. Yates, B. M. Hinds, and D. Eccleshall, Nucl. Phys. 44, 220 (1963).
⁷E. K. Warburton, P. Gorodetzky, and J. A. Becker, Phys. Rev. C 8, 418 (1973).
⁸J. W. Olness, E. K. Warburton, and J. A. Becker, Phys. Rev. C 7, 2239 (1973).
⁹J. C. Adloff, K. H. Souw, D. Disdier, F. Scheibling, P. Chevallier, and Y. Wolfson, Phys. Rev. C 10, 1819 (1974).
¹⁰J. C. Adloff, K. H. Souw, D. Disdier, and P. Chevallier, Phys. Rev. C 11, 738 (1975).
¹¹A. Gobbi, A. Ruh, B. Gobbi, and R. E. Pixley, Helv. Phys. Acta. 37, 104 (1964).
¹²R. W. Ollerhead, J. S. Lopes, A. R. Poletti, M. F. Thomas, and E. K. Warburton, Nucl. Phys. 66, 161 (1965).
¹³Z. Berant, M. B. Goldberg, M. Popp, J. S. Sokolowski, P. N. Tandon, and Y. Wolfson, Nucl. Phys. A173, 401 (1971).
¹⁴J. A. Becker, L. F. Chase, Jr., D. Kohler, and R. E. McDonald, Phys. Rev. C 8, 2007 (1973).
¹⁵J. S. Lopes, O. Häusser, R. D. Gill, and H. J. Rose, Nucl. Phys. 89, 127 (1966).
¹⁶R. Moreh, Nucl. Phys. A97, 106 (1967).
¹⁷J. L. Groh, R. P. Singhal, H. S. Caplan, and B. S. Dolbilkin, Can. J. Phys. 49, 2743 (1971).
¹⁸G. Bishop, in *Proceedings of the International Conference on Nuclear Physics, Munich, 1973*, edited by J. de Boer and H. J. Mang (North-Holland, Amsterdam/American Elsevier, New York, 1973), p. 459.
¹⁹P. Strehl, Z. Phys. 234, 416 (1970).
²⁰H. G. Benson and J. M. Irvine, Proc. Phys. Soc. Lond. 89, 249 (1966).
²¹I. Kanestroem and H. Koren, Nucl. Phys. A130, 527 (1969).
²²H. G. Benson and B. H. Flowers, Nucl. Phys. A126, 332 (1969).
²³D. H. Wilkinson, Nucl. Phys. A133, 1 (1969).